Compatibilization of Polypropylene/Polystyrene Blends with Poly(styrene-*b*-butadiene-*b*-styrene) Block Copolymer

GREGOR RADONJIČ,[1] VOJKO MUSIL,[1] IVAN ŠMIT[2]

[1]University of Maribor, EPF Maribor, Institute for Technology, Razlagova 14, 2000 Maribor, Slovenia

[2]Institute Ruđer Bošković, Bijenička 54, P.O. Box 1016, 10001 Zagreb, Croatia

Received 17 November 1997; accepted 13 February 1998

ABSTRACT: The compatibilizing effect of the triblock copolymer poly(styrene-*b*-butadiene-*b*-styrene) (SBS) on the morphology and mechanical properties of immiscible polypropylene/polystyrene (PP/PS) blends were studied. Blends with three different weight ratios of PP and PS were prepared and three different concentrations of SBS were used for investigations of its compatibilizing effects. Scanning electron microscopy (SEM) showed that SBS reduced the diameter of the PS-dispersed particles as well as improved the adhesion between the matrix and the dispersed phase. Transmission electron microscopy (TEM) revealed that in the PP matrix dispersed particles were complex "honeycomblike" aggregates of PS particles enveloped and joined together with the SBS compatibilizer. Wide-angle X-ray diffraction (WAXD) analysis showed that the degree of crystallinity of PP/PS/SBS slightly exceeded the values given by the addition rule. At the same time, addition of SBS to pure PP and to PP/PS blends changed the orientation parameters A_{110} and C significantly, indicating an obvious SBS influence on the crystallization process in the PP matrix. SBS interactions with PP and PS influenced the mechanical properties of the compatibilized PP/PS/SBS blends. Addition of SBS decreased the yield stress and the Young's modulus and improved the elongation at yield as well as the notched impact strength in comparison to the binary PP/PS blends. Some theoretical models for the determination of the Young's modulus of binary PP/PS blends were used for comparison with the experimental results. The experimental line was closest to the series model line. © 1998 John Wiley & Sons, Inc. J Appl Polym Sci 69: 2625–2639, 1998

Key words: compatibilization; mechanical properties; phase morphology; polymer blends; polypropylene blends; polystyrene blends; SBS block copolymer

INTRODUCTION

A satisfactory improvement of the mechanical properties of the polymer blend critically depends on the interfacial tension and the interfacial adhesion between the phases. In an immiscible polymer blend, like isotactic polypropylene/atactic polystyrene (iPP/aPS) blends, the adhesion between the phases is, in most cases, very weak. As a result, stress applied to the blend will not be transferred to the dispersed phase and, therefore, some mechanical properties are significantly lower than they would be as predicted by the weighted average of the properties of the components. Conversion of these phase-separated blends into useful polymeric materials with the combination of desirable properties of each component requires a modification of the interface.

Correspondence to: G. Radonjič.

Contract grant sponsors: Ministry of Science and Technology of Republic of Slovenia; Ministry of Science and Technology of Republic of Croatia.

Journal of Applied Polymer Science, Vol. 69, 2625–2639 (1998)

 CCC 0021-8995/98/132625-15

Lowering of interfacial tension leads to a smaller dispersed phase size,[1,2] and sufficient interfacial adhesion enables the matrix to withstand the stress and strains due to an applied load.[3,4] This can be achieved with the proper use of block or graft copolymers which act as interfacial agents.[5–7] The general criterion for the effective compatibilization with block copolymers is that each segment of the block copolymer interacts somehow with one of the blend components. Such compatibilizers should locate at the interface of two immiscible polymers and reduce the interfacial tension between the phases,[8,9] provide stability against coalescence, and result in improved interfacial adhesion.

Blending of polypropylene and polystyrene leads to brittle blends since they are thermodynamically immiscible.[10,11] Only a few studies were carried out to investigate the effectiveness of the poly(styrene-*b*-butadiene-*b*-styrene) (SBS) triblock copolymer as a compatibilizer for PP/PS blends. The effects of adding the SBS triblock copolymer to PP/PS blends when PS was a matrix phase were studied by Santana and Müller.[12] They reported that the morphology (the size of the dispersed PP particles) did not change when 2 wt % of SBS was added. This resulted in a lack of improvement in the tensile and impact properties of such blends. However, some differences in the crystallization behavior of PP in the blends containing SBS compared to those without SBS were observed. Compatibilization of high-impact polystyrene (PS-HI) and PP blends was studied by Horák et al.[13] The effect of di-, tri-, and pentablock types of styrene/butadiene block copolymers on the morphology and mechanical properties were studied. These authors showed obvious differences in appearance of the PS-HI/PP interfacial layer in the blends compatibilized with the diblock and those containing tri- or pentablock copolymers. Multiblock copolymers showed higher improvement in impact strength and elongation at break in comparison with the diblock copolymer. Recently, Fortelny and Michálková[14] studied the effect of the SBS compatibilizer as well as the rate and the time of mixing on the morphology of PP/PS blends with the weight ratio 75/25. They found that an admixture of the SBS copolymer led to the decrease in the average size of the dispersed PS particles, but, interestingly, it did not lead to an increase in the phase structure uniformity. Neither the increased rate of mixing nor the increased time of mixing resulted in a higher uniformity of the phase structure of the studied PP/PS blends. Hlavatá and Horák[15] also investigated the changes in crystallinity of PP in blends with PS-HI compatibilized with di- and triblock types of styrene/butadiene block copolymers. They concluded that the degree of crystallinity of PP in such blends did not change with the PS-HI content and slightly decreased when a styrenic block copolymer was added. Obieglo and Romer[16] showed how the addition of few percent of SBS can improve the notched impact strength of recycled PP/PS blends. A recent review of Datta and Lohse[17] confirmed that the compatibilization of PP/PS blends with SBS were not much studied.

It was found by other authors that SBS influences the mechanical properties of polymer blends. Ghaffar et al.[18] showed that SBS can be a very effective modifier for blends of low-density polyethylene (PE-LD) and PS. All measured mechanical properties (impact strength, tensile strength, elongation at break) were considerably improved. On the other hand, SBS was not so effective when other thermoplastics like PP or poly(vinyl chloride) were used instead of PS. Similar but not so evident improvements in the mechanical properties were found for ternary PE-LD/PP/PS blends modified with SBS.[19] Recently, two articles dealt with the role of SBS in blends of PP and high-density polyethylene (PE-HD).[20,21] The authors proposed different morphological models for such ternary blends depending on the processing conditions. They reported that with properly chosen processing conditions PP/PE-HD/SBS ternary blends with high impact resistance can be obtained.

In this article, we report on the investigations of the compatibilizing effects of SBS in immiscible PP/PS blends with the aim of correlating the morphology with the mechanical properties. Some theoretical models for the prediction of the Young's modulus of binary PP/PS blends were used and compared with the experimental values.

EXPERIMENTAL

Materials

The polymers used in this study were polypropylene Novolen 1100L (BASF), polystyrene GP-678E (DOKI), and poly(styrene-*b*-butadiene-*b*-styrene) Kraton D-1102 CS (Shell Chemical Co.) with a polystyrene/polybutadiene weight ratio 29/71. The polymers' characteristics are shown in Table I.

Table I Characteristics of Used Polymers

Material	M_w (g/mol)	M_w/M_n	MFI (g/10 min)	η (Pa s)	ρ (g/cm^3)
PP	435,420[a]	9.3	6.9[b]	680[d]	0.908[e]
PS	231,600[a]	2.4	12.5[c]	600[d]	1.05[e]
SBS	117,200[a]	1.7	6.6[c]	—	0.94[e]

[a]Measured by size-exclusion chromatography with PS standard.
[b]ASTM D 1238 (230°C/2.16 kg).
[c]ASTM D 1238 (200°C/5 kg).
[d]Data for 200°C, $\dot{\gamma} = 100\ s^{-1}$ (measured by Göttfert Rheograph capillary viscometer, $L/d = 20$).
[e]Manufacturer's data.

Blend Preparation

PS pellets were dried overnight at 70°C before use and premixed with PP and SBS pellets before being fed into the kneading chamber. Blends of different compositions were prepared by melt blending in oil-heated Brabender kneading chamber at 200°C for 6 min with a rotor speed of 50 rpm. After finishing the blending process, they were rapidly transferred between two aluminum sheets placed in the preheated hydraulic press at 220°C. Samples of blends used for investigations of the structure and mechanical properties were prepared by compression molding. The load of 100 bar was used, and after 10 min, the plates were moved out and cooled to room temperature in air. The weight ratios of PP and PS were 90/10, 70/30, and 50/50. The compatibilizer concentrations used were 2.5, 5, and 10 wt % for each PP/PS weight ratio.

Scanning Electron Microscopy (SEM)

A scanning electron microscope JEOL JSM-840A was used for studying the morphology. Samples were fractured in liquid nitrogen and covered with gold before being examined with the microscope at an acceleration voltage of 10 kV. To provide better insight into blend morphology, PS was etched in some samples with xylene from the sample surface at the room temperature. All SEM micrographs are secondary electron images.

Transmission Electron Microscopy (TEM)

Ultrathin sections (approximately 70-nm-thick) were cut at room temperature from 4-mm-thick plates with a Reichert-Jung Ultracut E microtome equipment with a diamond knife. Before microtoming, samples were exposed first to the OsO_4 vapor for 3 days. After that, overnight exposure to RuO_4 was performed due to the additional contrasting and hardening of the samples. Microtomed ultrathin sections were then placed on Cu grids and micrographs were taken at an acceleration voltage of 80 kV with a Phillips 3000 microscope.

Wide-Angle X-ray Diffraction (WAXD)

X-ray diffractograms of the samples (1-mm-thick plates) were taken by a Phillips PW 1050 diffractometer with monochromatized CuKα radiation. To compensate for the preferred orientation effect in the film plane, the samples were rotated during scanning over the diffraction range $2\theta = 4$–$50°$. Because of the broadened diffraction contribution from the PS and SBS amorphous phases, the degree of crystallinity (w_c) was evaluated by the Hermans–Weidinger method[22] using an angular range $2\theta = 6$–$34°$. Orientation parameters A_{110}, A_{130}, and C as measures for orientations of corresponding (110), (130), and (040) planes were calculated with formulas proposed by Trotignon and Verdu[23] and Zipper et al.[24,25] and defined by the following equations:

$$A_{110} = \frac{I_{110}}{I_{110} + I_{111} + I_{\bar{1}31+041}} \quad (1)$$

$$A_{130} = \frac{I_{130}}{I_{130} + I_{111} + I_{\bar{1}31+041}} \quad (2)$$

$$C = \frac{I_{040}}{I_{110} + I_{040} + I_{130}} \quad (3)$$

where I represents the intensities of the corresponding reflections. From a half-maximum width of 110, 130, and 040 reflections, the crystallite sizes L_{110}, L_{130}, and L_{040} were calculated using the Scherrer formula[26] after the correction

for instrumental broadening with a 111 germanium diffraction profile.

Mechanical Testing

Test specimens for the tensile measurements were prepared from 1-mm-thick plates according to ASTM D 638. The Young's modulus, yield stress, and elongation at yield were measured by a tensile tester Frank 81105 at 23°C with six specimens for each sample. The strain rate was 1 mm/min. The test specimens for the notched impact strength were cut from 4-mm-thick compression-molded plates. Testing bars were then machined to the dimensions of 50 × 6 × 4 mm. A U-shaped notch was cut at the center of each specimen with a depth of 1.3 mm. Specimens were fractured according to the Charpy test on the Frank apparatus with a 0.5 J weight at 23°C (DIN 53453). Ten test specimens for each sample were measured.

RESULTS AND DISCUSSION

Phase Morphology

Electron Microscopy Observations

SEM micrographs of binary PP/PS blends shown in Figure 1 demonstrate a two-phase morphology, indicating immiscibility of the components. Increasing the amount of PS results in bigger and coarser PS particles. When the weight percents of PP and PS are equal, the cocontinuous morphology is observed [Fig. 1(c)]. This is in accordance with some morphological models[27] which predict the occurrence of a cocontinuous phase morphology on the basis of the viscosity ratio of the components. In Figure 1(c), the PS phase is etched with xylene to obtain better insight into the blend morphology. Morphological studies provide evidence for interfacial activity of block copolymers. Figure 2 shows SEM micrographs of fractured surfaces of PP/PS blends with the same PP/PS weight ratios as in Figure 1 but containing 5 wt % of the SBS compatibilizer. Again, PS and SBS were etched with xylene. The size of the dispersed PS particles is reduced upon the addition of the SBS triblock copolymer. The reduction is especially evident in the PP/PS/SBS 85.5/9.5/5 blend [Fig. 2(a)], where the PS particles have diameters of submicron sizes. A smaller average interfacial area of PS particles compared to the blend with 30 wt % of PS is the reason for the more efficient

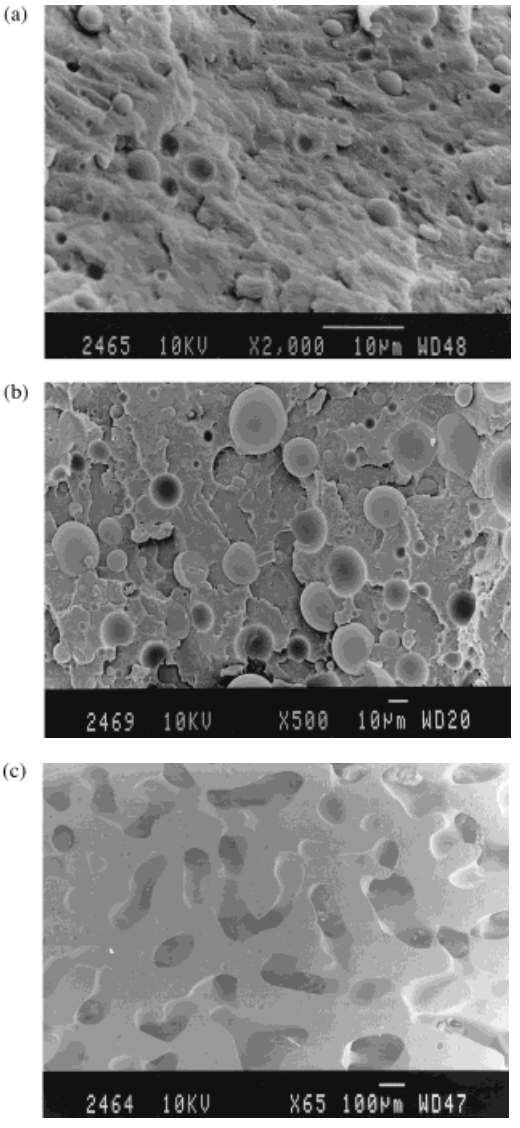

Figure 1 Scanning electron micrographs of phase morphologies of noncompatibilized PP/PS blends with different weight ratios: (a) 90/10; (b) 70/30; (c) 50/50 (PS etched with xylene). Note different magnifications.

interfacial activity of SBS at this level of concentration. The cocontinuous morphology of the ternary 47.5/47.5/5 blend [Fig. 2(c)] is quite different from the morphology of the binary PP/PS 50/50 blend [Fig. 1(c)]. Areas of cocontinuity in the ternary PP/PS/SBS 47.5/47.5/5 blend can be seen in Figure 2(c), but on a much finer scale than those for the binary PP/PS 50/50 blend in Figure 1(c). Probably not only the reduction of interfacial tension but also the distribution of SBS in two homopolymer phases change the viscosity ratio and influence the morphology development. A higher magnification of the morphology of the PP/PS

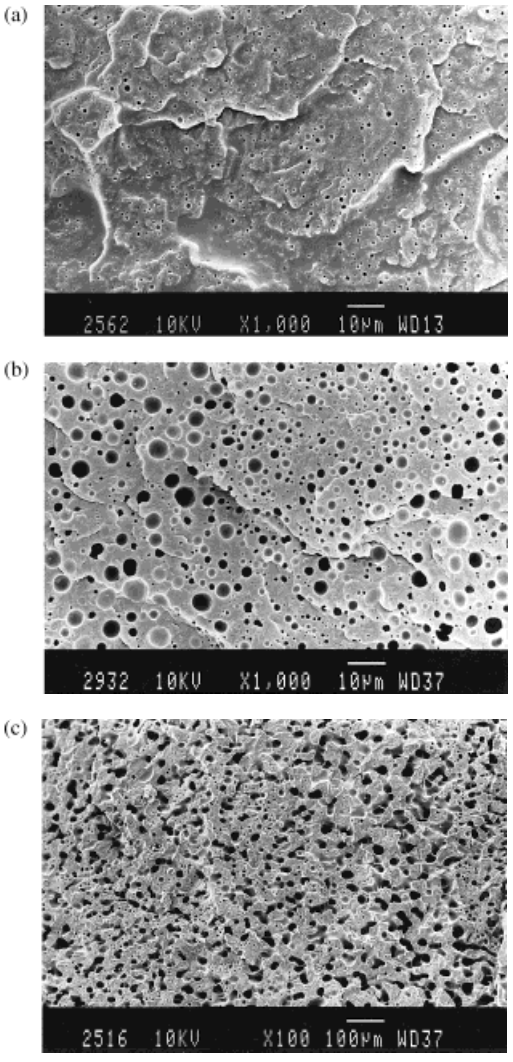

Figure 2 Scanning electron micrographs of phase morphologies of compatibilized PP/PS blends with 5 wt % of SBS with different PP/PS weight ratios: (a) 90/10; (b) 70/30; (c) 50/50 (PS and SBS etched with xylene). Note different magnifications.

70/30 blend compatibilized with 10 wt % of SBS is shown in Figure 3. Dispersed particles are strongly embedded in the PP matrix. Their surfaces after fracture are not smooth, indicating good adhesion. An interfacial layer can be observed around each particle without any voids between the particles and matrix.

Direct evidence of the interfacial activity of the SBS triblock copolymer and improved interfacial adhesion is further confirmed in Figure 4. The fractured surface with a PS particle is covered with a layer of the compatibilizer spreading from the particle surface into the matrix phase with fibrils which hold the particle in the matrix. Such

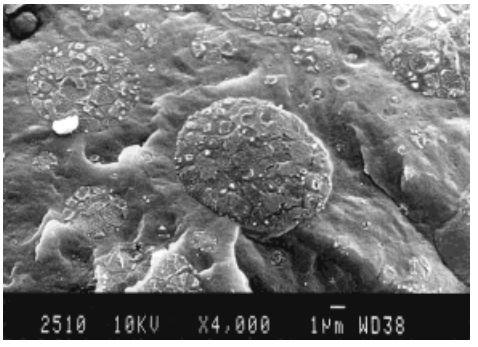

Figure 3 Scanning electron micrograph of phase structure of compatibilized PP/PS 70/30 blend containing 10 wt % of SBS compatibilizer. An interfacial layer which envelopes each dispersed particle can be observed.

improved interfacial adhesion enables the applied stress to be transferred also through the dispersed phase. An effect of such stress transfer is shown in Figure 5 where the fractured surface with a broken PS particle can be seen embedded strongly in PP matrix and covered with an interfacial layer. The breaking of the dispersed PS particles can participate in additional energy dissipation which can contribute to better impact properties.

Additional insight into the blends' morphology and SBS interfacial activity was obtained by transmission electron microscopy (TEM). Figure 6 shows the morphology of the PP/PS blends with a weight ratio 70/30 compatibilized with 10 wt % of SBS. Unsaturated parts, for example, polybutadiene (PB) blocks in SBS, were selectively

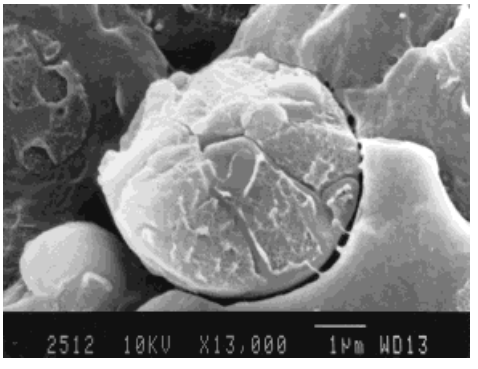

Figure 4 Scanning electron micrograph of the fractured surface of PP/PS 70/30 blend compatibilized with 5 wt % of SBS showing the PS particle covered with a layer of the SBS compatibilizer. Fibrils which connect both phases after the fracture show improved interfacial adhesion.

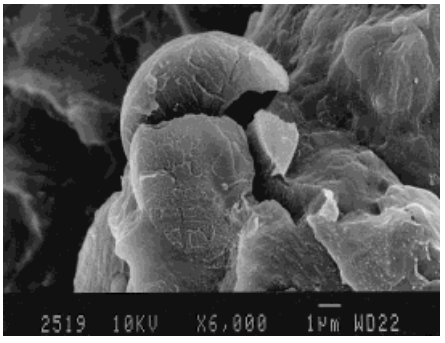

Figure 5 Scanning electron micrograph of the fractured surface of PP/PS 70/30 blend compatibilized with 2.5 wt % of SBS. A broken PS particle is covered with a layer of the SBS compatibilizer showing an effect of the transferred stress from the matrix to the dispersed phase.

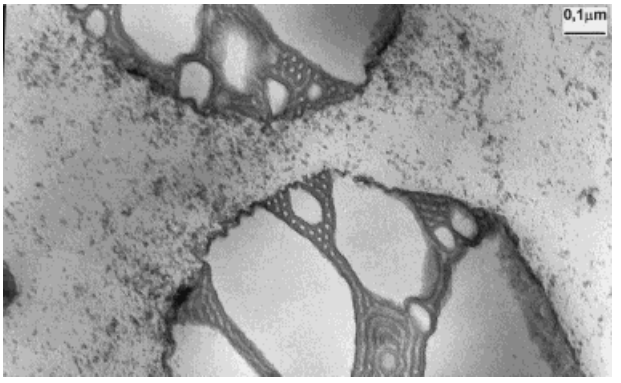

Figure 7 Transmission electron micrograph of PP/PS 70/30 blend compatibilized with 10 wt % of SBS and stained with OsO_4 and RuO_4 showing SBS interfacial layers around and inside the dispersed aggregates (scale bar represents 0.1 μm).

contrasted by OsO_4 and RuO_4 vapor and appear dark gray or black. PS blocks of SBS and pure PS remained brighter on this micrograph. TEM analysis revealed that SBS is not only located at the interphase between the PP and PS phases where it lowers the interfacial tension as well as improves the adhesion between both phases but forms, together with pure PS dispersed particles, a complex structure. Figure 6 shows that the dispersed particles in the PP matrix are aggregates of PS particles, which are surrounded and joined together with the SBS triblock copolymer. Moreover, small black particles inside the PP matrix on the micrograph in Figure 6 are probably residual dispersed SBS. Such dispersed SBS particles can, for example, contribute to the improved notched impact strength of the PP/PS/SBS blends. A higher magnification of the morphology of the compatibilized PP/PS 70/30 blend with 10 wt % of SBS is shown in Figure 7. The phase boundary between the PP matrix and the SBS interfacial layer around the dispersed particles is not smooth but diffuse. This is due to the inter-

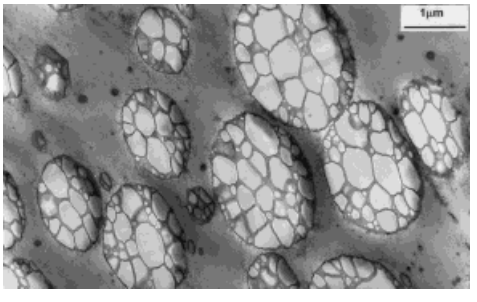

Figure 6 Transmission electron micrograph of PP/PS 70/30 blend compatibilized with 10 wt % of SBS and stained with OsO_4 and RuO_4 (scale bar represents 1 μm).

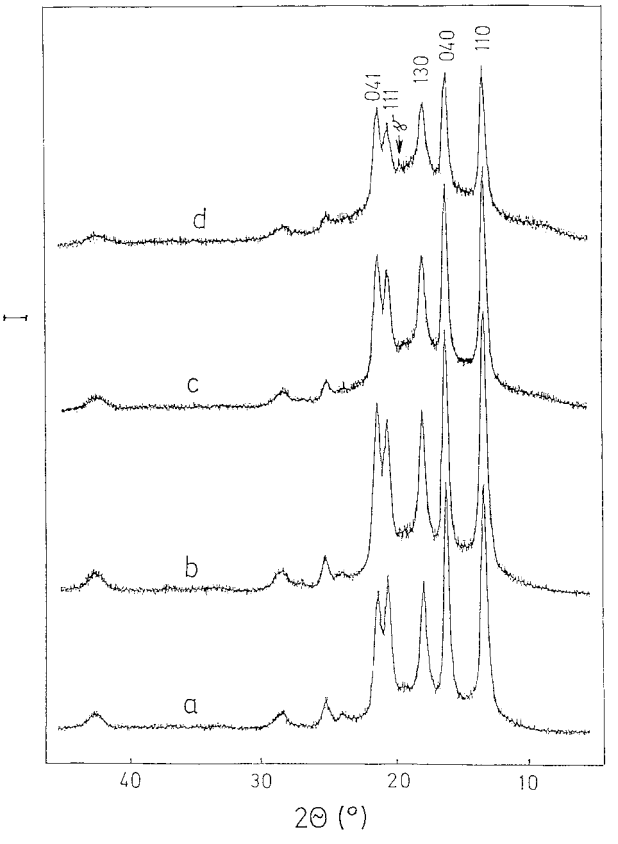

Figure 8 Diffractograms of (a) pure PP and PP/PS blends with different weight ratios: (b) 90/10; (c) 70/30; (d) 50/50.

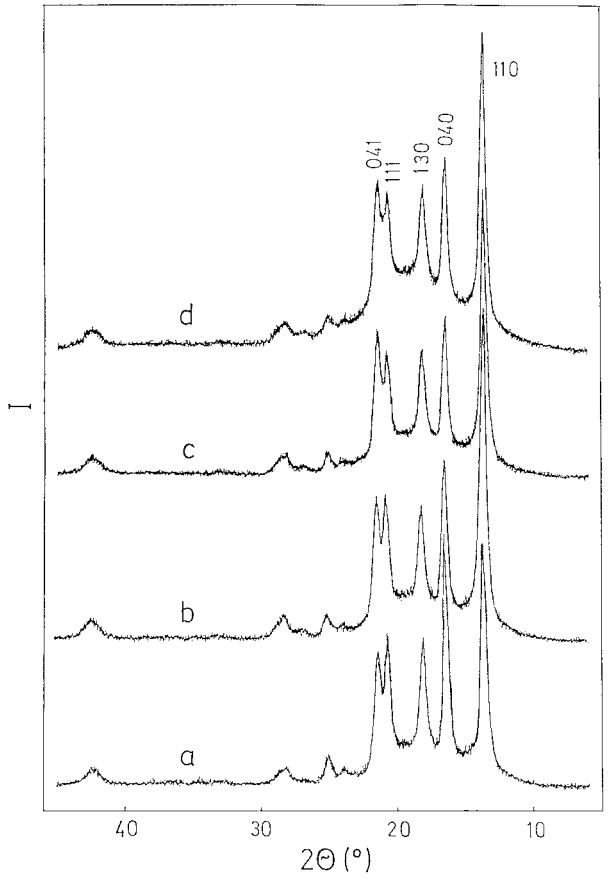

Figure 9 Diffractograms of (a) pure PP and PP/SBS blends with different weight ratios: (b) 95/5; (c) 90/10; (d) 70/30.

diffusion between the PP chains and PB blocks of the SBS block copolymer at the interphase. A major amount of SBS is located inside the dispersed particles, where they connect pure PS particles. SBS is, at room temperature, a phase-separated linear thermoplastic elastomer with two PS endblocks which form domains of different morphologies (depending on PS content) and a central PB block.[28] As shown in Figure 7, in dispersed aggregates, the SBS layers which surround the pure PS particles mostly preserve the phase-separated morphology. It can be seen that PS blocks of SBS form spherical or layered domains, but obviously penetrate also into each of pure PS particles and, therefore, join them into complex aggregates with a "honeycomblike" morphology.

Horák et al.[13] showed by TEM of the PS-HI/PP blends compatibilized with SBS that SBS was present in the PP phase as well as in the PS-HI phase as small particles but it also formed an interfacial layer between PP and PS-HI. Recently, Zhang et al.[21] observed for PP/PE-HD/SBS blends complex morphologies of dispersed particles composed of PE-HD and SBS. They reported that the formation of such a complex particle morphology is very much dependent on the processing parameters.

In our previous studies[29–31] on the compatibilization of the PP/PS blends, even larger reductions in the size of the dispersed PS phase in immiscible PP/PS blends were obtained by the addition of the poly(styrene-*b*-ethylene-*co*-propylene) (SEP) diblock copolymer. This resulted in significant improvement in the notched impact strength. But it has to be pointed out that it is not necessarily that the diblock copolymer is superior as an interfacial agent compared to the triblock copolymer.[13,32,33] Our morphological observations are in accordance with the observations of the already-mentioned studies of Fayt et al.[2,3] It is believed that triblock copolymers have conformational restraints, whereas each segment of a

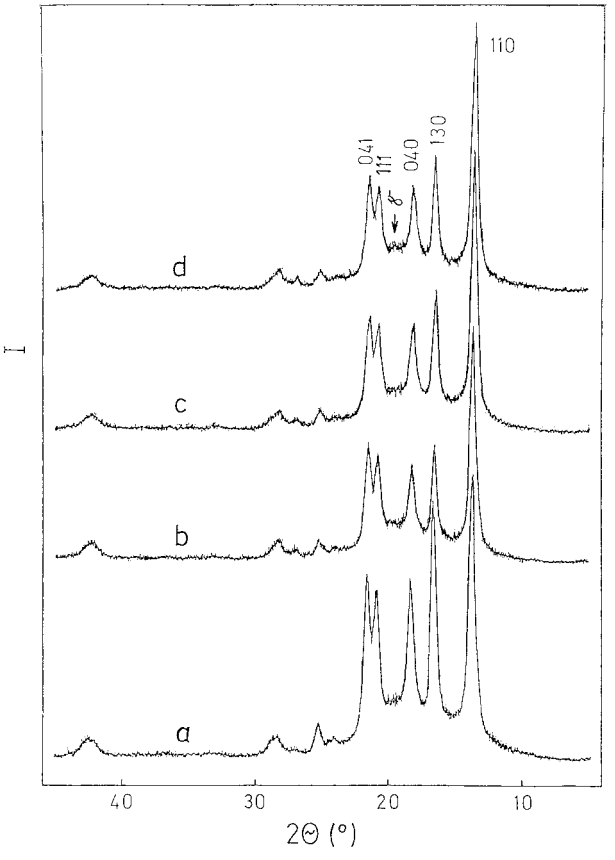

Figure 10 Diffractograms of PP/PS 90/10 blends compatibilized with (a) 0 wt % SBS, (b) 2.5 wt % SBS, (c) 5 wt % SBS, and (d) 10 wt % SBS.

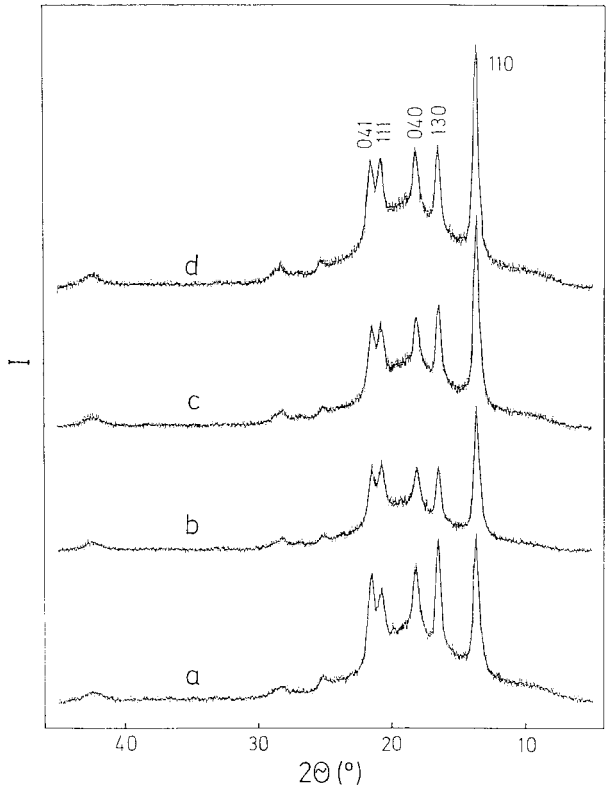

Figure 11 Diffractograms of PP/PS 50/50 blends compatibilized with (a) 0 wt % SBS, (b) 2.5 wt % SBS, (c) 5 wt % SBS, and (d) 10 wt % SBS.

diblock copolymer penetrates more easily in a particular homopolymer phase.

Wide-Angle X-ray Diffraction

The influences of SBS and PS on the phase structure of the iPP matrix were studied by WAXD. The diffractograms of all samples mainly exhibit peaks of the stable monoclinic α-form of the iPP crystalline phase. The diffractograms of iPP are given in Figures 8(a) and 9(a), of binary PP/PS blends in Figure 8(b–d), of binary PP/SBS blends in Figure 9(b–d), and of ternary PP/PS/SBS blends with PP/PS weight ratios 90/10 and 50/50 compatibilized with 2.5, 5, and 10 wt % of SBS in Figures 10 and 11. A hardly noticeable 117 peak on the diffractogram of the binary PP/PS 50/50 blend in Figure 8(d) indicates the possibility of the appearance of a trace of the iPP γ-form with the addition of PS. Although the metastable β-form may appear by adding different nucleating agents like SBS or PS,[34] the 003 reflection of the β-form does not appear in any of diffractograms of the binary and ternary blends.

Ternary PP/PS/SBS blends with a low amount of SBS (2.5 wt %) show a slight increase of the degree of crystallinity (w_c) as shown in Figure 12. While the crystallinity of the binary PP/PS blends decreases according to the addition rule, the crystallinity of the ternary PP/PS/SBS blends exceeds the values given by the addition rule (data in ref. 35).

The most expressed difference between the PS and SBS effects on the crystalline iPP phase is observed in the reflection intensity, that is, the orientation of the iPP crystallites. While the addition of the PS component did not change the intensity ratio of the crystalline peaks (in Fig. 8, the diffractograms of PP/PS blends with different weight ratios are similar except the reflections in doublet), the addition of only the 2.5 wt % SBS compatibilizer significantly increases the 110 reflection and supresses the 040 reflection in ternary PP/PS/SBS blends (Figs. 10 and 11) as well as in binary PP/SBS blends (Fig. 9). Such effects are reflected in the corresponding orientation parameter values. The orientation parameter A_{110}

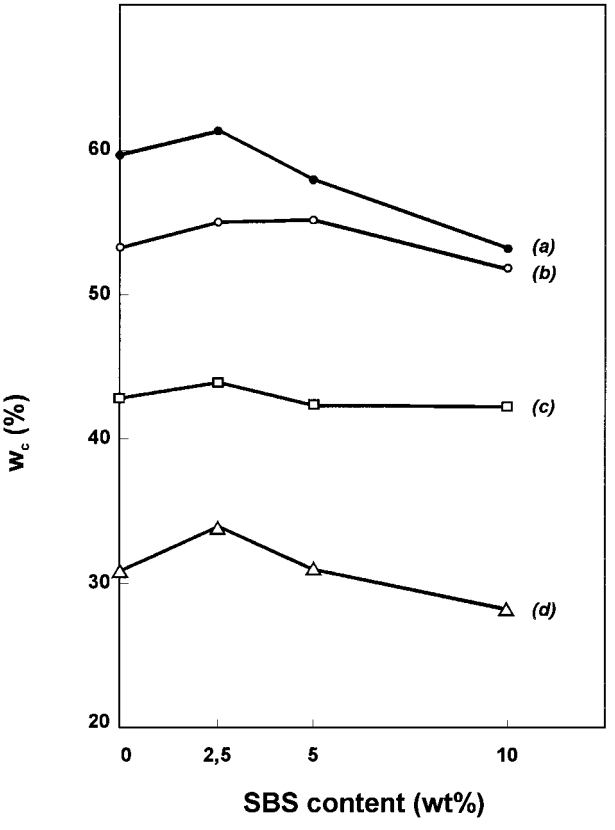

Figure 12 Crystallinity (w_c) dependence of SBS weight content for PP/PS blends with different weight ratios: (a) 100/0; (b) 90/10; (c) 70/30; (d) 50/50.

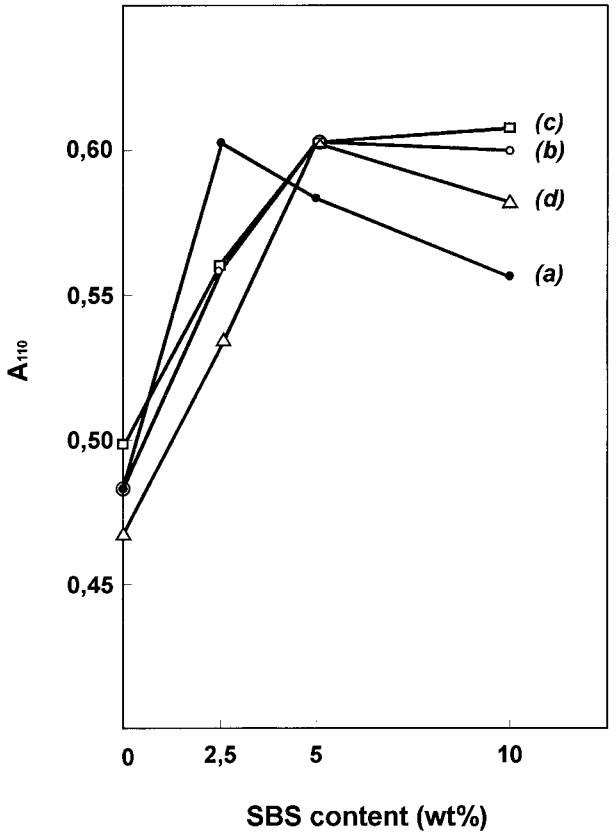

Figure 13 Orientation parameter A_{110} dependence of SBS weight content for PP/PS blends with different weight ratios: (a) 100/0; (b) 90/10; (c) 70/30; (d) 50/50.

increases significantly with SBS addition (Fig. 13), but at the same time, the orientation parameter C decreases (Fig. 14) for all blends. Such a change in orientation behavior, that is, increase of the crystal (110) planes, as well as decrease of (040) planes parallel to the sample surface, indicates an obvious reorientation influence of SBS in the crystallization process of the PP matrix. We also observed that the orientation parameter A_{130} as well as the crystallite size L_{130} did not differ significantly for all the samples.

Figures 15 and 16 show the SBS content dependence of the crystallite sizes L_{110} and L_{040}, respectively. While the crystallite size L_{110} has a constant value in the case of binary PP/SBS and ternary PP/PS/SBS blends with the weight ratio of PP and PS of 90/10, it increases for the blends with a higher amount of PS (30 and 50 wt %), as shown in Figure 15. The crystallite size L_{040} shows a maximum when 2.5 wt % of SBS is added to the blends with different PP/PS weight ratios. However, L_{040} decreases with the addition of SBS to the pure PP. This is shown in Figure 16. From Figures 15 and 16, we can conclude that the crystallite sizes L_{110} and L_{040} are rather influenced by the PS component (or by the combined effects of PS and SBS) than by the SBS triblock copolymer alone.

In this manner, while the crystallinity orientation parameters A_{110} and C are influenced mainly by the SBS triblock copolymer, the crystallite sizes are influenced predominantly by the PS component. Such behavior indicates an obvious effect of the SBS interlayer and/or SBS particles dispersed in the PP matrix on the crystallization process in the PP matrix of compatibilized PP/PS/SBS blends. On the other hand, the influence of the PS phase can be explained by different phase morphologies of the PP/PS blends with different PP/PS weight ratios (supported by ref. 35).

Mechanical Properties

Stress–Strain Behavior

Stress–strain curves in the yield region of homopolymers, binary PP/PS blends, and ternary

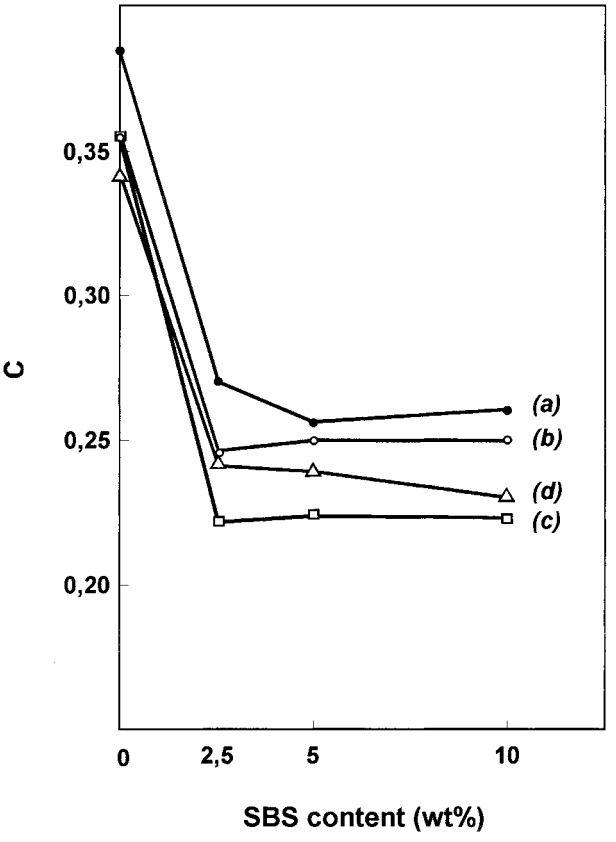

Figure 14 Orientation parameter C dependence of SBS weight content for PP/PS blends with different weight ratios: (a) 100/0; (b) 90/10; (c) 70/30; (d) 50/50.

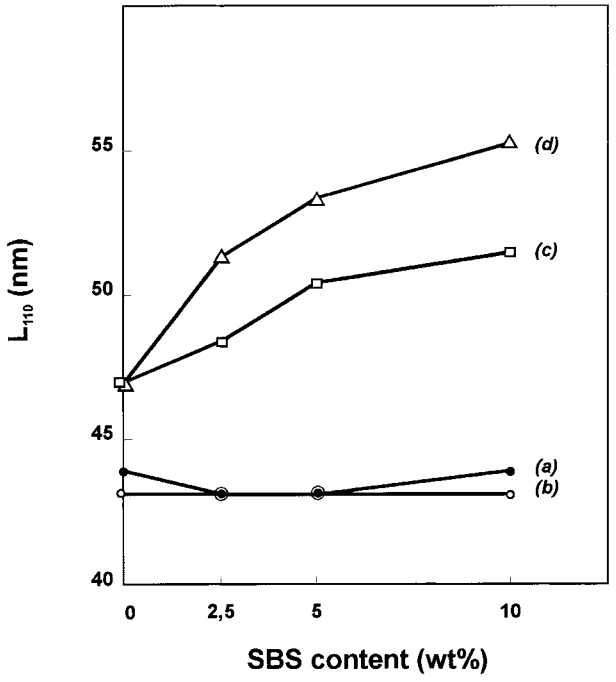

Figure 15 Crystallite size (L_{110}) dependence of SBS weight content for PP/PS blends with different weight ratios: (a) 100/0; (b) 90/10; (c) 70/30; (d) 50/50.

PP/PS/SBS blends are shown in Figure 17. Polypropylene is a ductile polymer and the incorporation of a second polymer in the PP matrix often results in a decreased yield stress as well as a lower elongation at yield and elongation at break.[33,36] The yield stress of binary PP/PS blends decreases with an increasing amount of PS. PS particles behave as voids and, therefore, reduce the effective load-bearing cross section which decreases the yield stress of binary PP/PS blends. The yield point of the noncompatibilized PP/PS 90/10 blend is relatively sharp and distinct in comparison to the compatibilized PP/PS 90/10 blends [Fig. 17(b)]. This distinction becomes stronger with the increasing amount of the added compatibilizer. Binary blends with a PP/PS weight ratio of 70/30 and 50/50 fracture in a brittle manner [Fig. 17(c,d)]. When SBS is added, blends become less stiff and their elongation at yield increases compared to the binary PP/PS blends [Fig. 17(b–d)].

Variations of the yield stress and elongation at yield as a function of the compatibilizer content and different weight ratios of PP and PS are shown in Figures 18 and 19. Yield stress decreases with increasing SBS concentration (Fig. 18) in a similar fashion to the degree of crystallinity changes in Figure 12, that is, with a tendency of the maximum forming at the lower SBS content. This similarity indicates that the yield stress of compatibilized PP/PS/SBS blends is determined primarily by the degree of crystallinity, that is, by the rigidity of the PP matrix. On the other hand, elongation at yield increases as the concentration of SBS increases as shown in Figure 19. This effect is more evident for blends with a higher amount of PS. The improvement of elongation at yield with the addition of SBS can be attributed to the reduction of the particle size and improved interfacial adhesion. In our previous studies,[29–31] we did a more detailed analysis of the yield stress data for binary PP/PS blends as a function of their composition on the basis of some theoretical models.

Young's Modulus

The Young's modulus of the blends as a function of SBS content and the PP/PS weight ratio is shown in Figure 20. Binary PP/PS blends have a bit higher Young's modulus than that of pure PP which has a value of 1820 N/mm^2. This stiffness effect could be the result of differences in the thermal expansion coefficients of PP and PS.[37] As it is cooled from the melt temperature, the PP

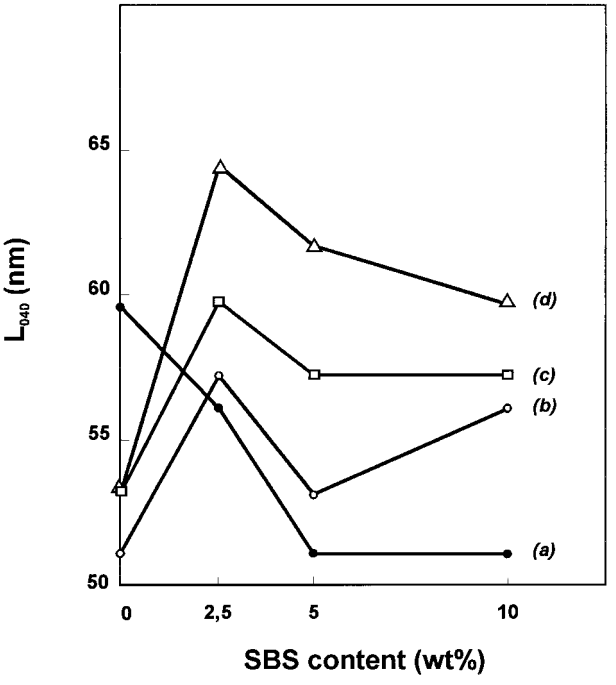

Figure 16 Crystallite size (L_{040}) dependence of SBS weight content for PP/PS blends with different weight ratios: (a) 100/0; (b) 90/10; (c) 70/30; (d) 50/50.

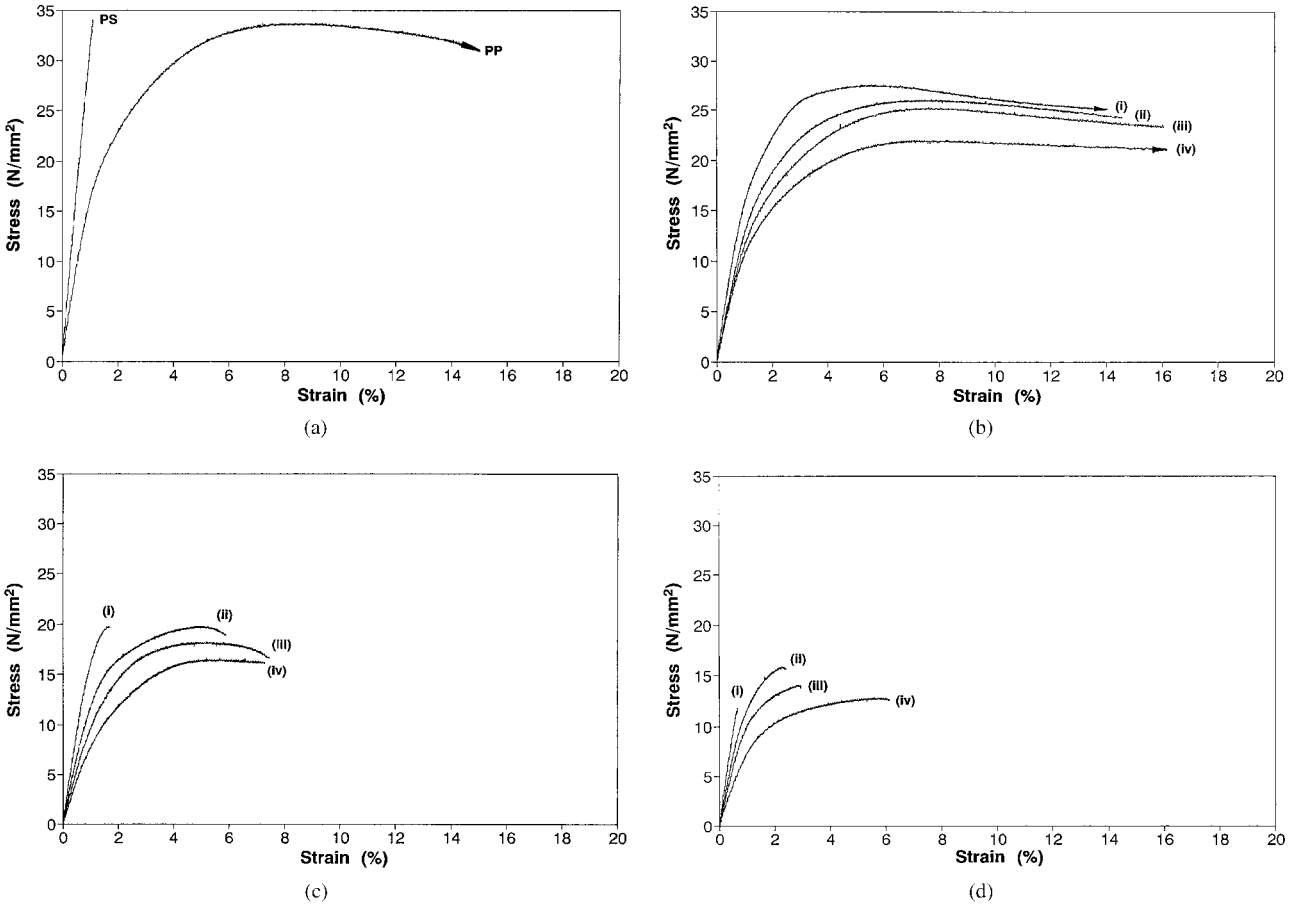

Figure 17 Stress–strain curves in the yield region of (a) PP and PS homopolymers and noncompatibilized and compatibilized PP/PS blends with different weight ratios: (b) 90/10; (c) 70/30; (d) 50/50; (i) without SBS; (ii) 2.5 wt % SBS; (iii) 5 wt % SBS; (iv) 10 wt % SBS. Test temperature 23°C; strain rate 1 mm/min.

matrix shrinks more, tightly embedding the PS phase. The measured value of the Young's modulus for pure PS is 3270 N/mm^2. Therefore, there is no significant participation of PS to the overall rigidity for binary PP/PS blends. The Young's modulus of binary PP/PS blends increases slightly as the PS concentration increases. But as the values for the binary blends are much closer to pure PP than to PS even at the cocontinuity region, it is evident that the PP matrix contributes the main part to the binary blends' rigidity. With increasing concentration of the SBS, the values of the Young's modulus decrease gradually. Thermoplastic elastomers usually lower the blend stiffness due to their elastomeric nature.[4,13,38] As seen in Figure 20, there is not a big difference in the Young's modulus values for compatibilized blends with PP/PS weight ratios of 70/30 and 50/50.

Various models exist for the prediction of the modulus–concentration dependence of two-phase polymeric materials.[39,40] The two simplest models are the so-called parallel and series models which should represent the upper and lower bounds of the Young's modulus predictions.[39] A parallel model, which assumes a uniform strain, is given by the equation

$$E_b = E_m\phi_m + E_d\phi_d \tag{4}$$

and a series model, which assumes a uniform stress, by equation

$$\frac{1}{E_b} = \frac{\phi_m}{E_m} + \frac{\phi_d}{E_d} \tag{5}$$

where E is the Young's modulus, and ϕ, the volume fraction. The subscript b denotes the blend,

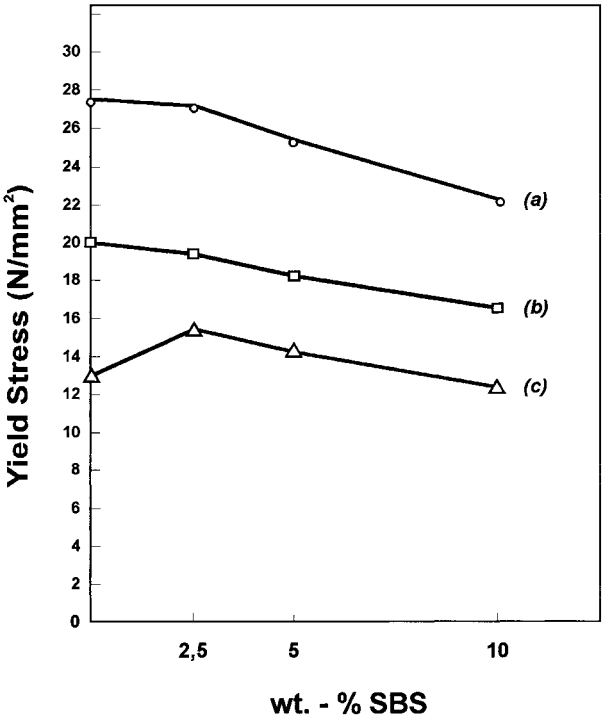

Figure 18 Yield stress as a function of SBS weight content and PP/PS weight ratio: (a) 90/10; (b) 70/30; (c) 50/50.

m denotes the matrix, and d denotes the dispersed phase.

One of the most widely used approximate expressions is that developed by Kerner.[41] Kerner's equation relies on the assumption that the dispersed-phase particles are spherical, the system is isotropic, and the adhesion between the two phases is perfect. The Young's modulus is then given by the following equation:

$$\frac{E_b}{E_m} = \frac{\dfrac{\phi_d E_d}{(7-5\nu_m)E_m + (8-10\nu_m)E_d} + \dfrac{\phi_m}{15(1-\nu_m)}}{\dfrac{\phi_d E_m}{(7-5\nu_m)E_m + (8-10\nu_m)E_d} + \dfrac{\phi_m}{15(1-\nu_m)}} \quad (6)$$

where ν_m is the Poisson ratio of the matrix. In our calculations, the value of 0.35 for the Poisson ratio for PP was used. The Kerner equation can be greatly simplified in some cases[39] assuming that the modulus of the dispersed phase does not contribute to the blend modulus. Such a case exists when adhesion between two phases is completely absent and inclusions are embedded loosely in the holes of the matrix phase. Such inclusions cannot give any contribution to the overall blend modulus since no stress can be transmitted across the interface. Hence, only the matrix contributes to the observed blend modulus. Assuming $E_d \approx 0$, eq. (6) simplifies to

$$\frac{E_b}{E_m} = \frac{1}{1 + \dfrac{\phi_d}{\phi_m}\left[\dfrac{15(1-\nu_m)}{7-5\nu_m}\right]} \quad (7)$$

Sato and Furukawa[42] derived an equation for the modulus of a two-phase system in which ellipsoidal cavities are formed during matrix deformation at the poles of each dispersed particle. They introduced the parameter τ which is equal to 0 in case of perfect adhesion and equal to 1 for the system with no adhesion at the boundary where

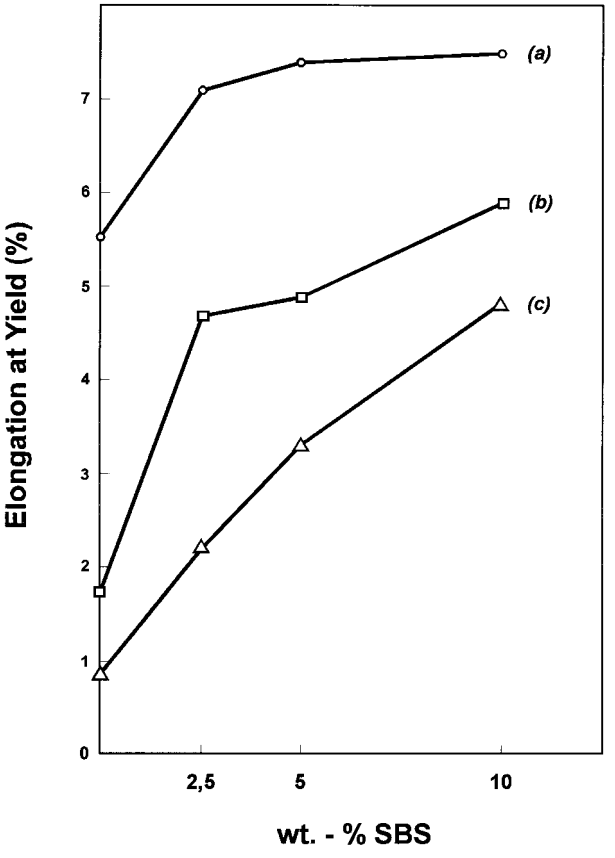

Figure 19 Elongation at yield as a function of SBS weight content and PP/PS weight ratio: (a) 90/10; (b) 70/30; (c) 50/50.

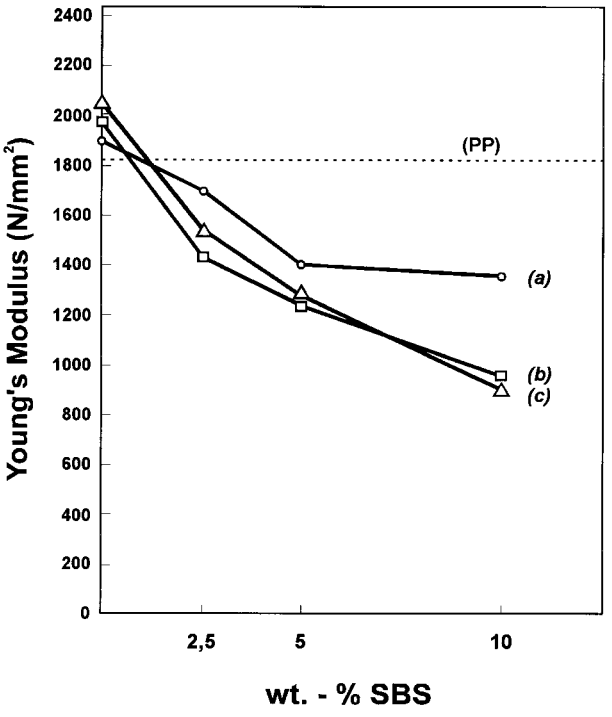

Figure 20 Young's modulus as a function of SBS weight content and PP/PS weight ratio: (a) 90/10; (b) 70/30; (c) 50/50.

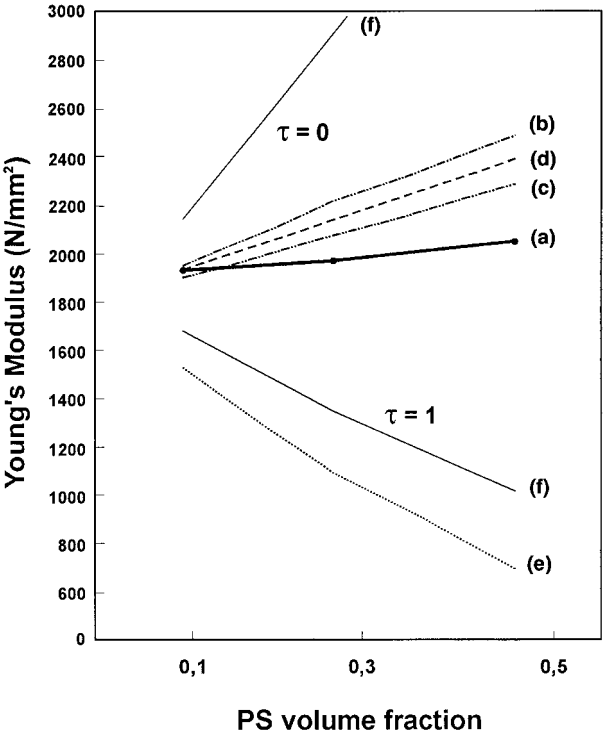

Figure 21 Young's modulus of PP/PS blends as a function of PS volume fraction compared to theoretical predictions, calculated by eqs. (4)–(8): (a) experimental line; (b) parallel model; (c) series model; (d) Kerner model; (e) simplified Kerner model; (f) Sato–Furukawa model.

cavities occur. Their equation has the following form:

$$\frac{E_b}{E_m} = \left[1 + \frac{y^2}{2(1-y)}\right]\left[1 - \frac{y^3\tau}{3}\left(\frac{1+y-y^2}{1-y+y^2}\right)\right] - \frac{y^2\tau}{3(1-y)}\left[\frac{1+y-y^2}{1-y+y^2}\right] \quad (8)$$

where the concentration variable y is defined as $y = \phi^{1/3}$.

Figure 21 shows the experimental blend modulus compared to the theoretical values calculated by the described models [eqs. (4)–(8)]. Comparison of the experimental and theoretical results for the PP/PS 90/10 blends is excellent for the different models used in this study. As the concentration of PS increases (30 and 50 vol %), the deviation from the theoretical values becomes evident. The slope of the experimental line is less steep compared to simple lower-bound values [calculated by eq. (5)], showing that PP still contributes a major part to the blend stiffness. A similar trend was observed by Kunori and Geil[43] in their work on polycarbonate and PE-HD blends although such behavior is not typical for immiscible blends. This trend

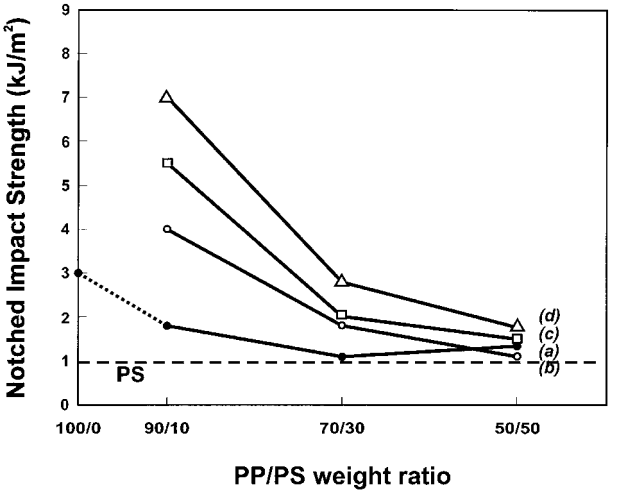

Figure 22 Notched impact strength at the room temperature as a function of PP/PS weight ratio and SBS weight content: (a) without SBS; (b) 2.5 wt % SBS; (c) 5 wt % SBS; (d) 10 wt % SBS.

might change with the different types of PP and PS used.[29,30]

Impact Resistance

In Figure 22, the notched impact strength of the blends at room temperature is plotted as a function of the PP/PS weight ratio and SBS content. Noncompatibilized blends have poorer impact properties compared to pure PP. The addition of SBS improves the impact resistance of the blends, especially in the case of the 90/10 blend. With an increasing amount of PS, the notched impact strength evidently decreases. PP/PS blends with a 50/50 weight ratio remain brittle no matter how much SBS is added. The main reasons for the improved impact behavior in the case of lower PS content are the reduction of the PS particle size and better interfacial adhesion. The improvement of the notched impact strength is probably not due entirely to the interfacial activity of SBS. The TEM micrograph in Figure 6 shows that some amount of the added SBS is dispersed in the PP matrix where it can act as an impact modifier, namely, it is well known that thermoplastic elastomers are very efficient toughening agents.[44] Additionally, SBS has an effect on the crystallization process of the PP matrix, and by changing of structural characteristics of PP, especially the spherulite size,[45] it can contribute to higher toughness. From Figure 22, it can be concluded that SBS, even in low amounts, contributes to improvements in impact resistance when the PP/PS weight ratio is 90/10 or 70/30, but all blends with a PP/PS 50/50 weight ratio have poor notched impact strength.

CONCLUSIONS

The results confirmed the immiscibility of binary blends of PP and PS with a phase-separated morphology. The triblock copolymer SBS acts as an effective compatibilizing agent for PP/PS blends as well as influences the crystallization process in the PP matrix. The following conclusions can be summarized:

1. The SBS interlayer envelopes PS particles and shows multiple activity with both phases:
   - As an interfacial agent between the PP matrix and the dispersed PS particles, it lowers the interfacial tension and improves the interfacial adhesion.
   - It diminishes the coalescence of PS particles and reduces the average particle size of the dispersed PS.
   - It envelopes small PS particles and connects them into complex PS/SBS aggregates with a "honeycomblike" morphology.
2. SBS interlayers and dispersed SBS particles in the PP matrix affect the crystallization process of PP, influencing the crystallinity and crystallite orientation.

Obviously, SBS does not act only as a compatibilizing agent between the PP and PS phases, but also affects the phase morphology of both the PP and PS components. As a result of the SBS interfacial activity, the notched impact strength and elongation at yield of the ternary PP/PS/SBS blends are improved in comparison to the binary PP/PS blends. A comparison of the experimental values of the Young's modulus of the binary PP/PS blends with some theoretical predictions showed that the experimental line is the closest to the series model line.

This work was supported by the Ministry of Science and Technology of the Republic of Slovenia and the Ministry of Science and Technology of the Republic of Croatia. The authors also wish to thank Mr. J. Pohleven for his help in the preparation of the samples. TEM micrographs were made at the Technical University Graz, Austria, with the technical assistance of Dr. E. Ingolic. We thank Mrs. M. Šmitek from Shell Slovenia for providing us with the Kraton block copolymers.

REFERENCES

1. Y. Takeda and D. R. Paul, *J. Polym. Sci. Polym. Phys.,* **30,** 1273 (1992).
2. R. Fayt, R. Jerôme, and Ph. Teyssié, *Makromol. Chem.,* **187,** 837 (1986).
3. R. Fayt, R. Jerôme, and Ph. Teyssié, *J. Polym. Sci. Polym. Phys.,* **27,** 775 (1989).
4. J. Rösch and R. Mülhaupt, *Makromol. Chem. Rapid Commun.,* **14,** 503 (1993).
5. L. A. Utracki, *Polymer Alloys and Blends: Thermodynamics and Rheology,* Hanser, Munich, Vienna, New York, 1989, Chap. 2.
6. D. R. Paul, in *Polymer Blends,* Vol. 2, D. R. Paul and S. Newman, Eds., Academic Press, New York, 1978, Chap. 12.

7. N. G. Gaylord, *J. Macromol. Sci. Chem. A,* **26,** 1211 (1989).
8. J. Noolandi and K. M. Hong, *Macromolecules,* **15,** 482 (1982).
9. T. A. Vilgis and J. Noolandi, *Makromol. Chem. Macromol. Symp.,* **16,** 225 (1988).
10. S. Krause, in *Polymer Blends,* Vol. 1, D. R. Paul and S. Newman, Eds., Academic Press, New York, 1978, Chap. 2.
11. L. A. Utracki and M. M. Dumoulin, in *Polypropylene: Structure, Blends and Composites,* Vol. 2, J. Karger-Kocsis, Ed., Chapman and Hall, London, 1995, Chap. 3.
12. O. O. Santana and A. J. Müller, *Polym. Bull.,* **32,** 471 (1994).
13. Z. Horák, V. Fort, D. Hlavatá, F. Lednicky, and F. Večerka, *Polymer,* **37,** 65 (1996).
14. I. Fortelny and D. Michálková, *Polym. Networks Blends,* **7,** 125 (1997).
15. D. Hlavatá and Z. Horák, *Eur. Polym. J.,* **30,** 597 (1994).
16. G. Obieglo and K. Romer, *Kunststoffe,* **83,** 926 (1993).
17. S. Datta and D. J. Lohse, *Polymeric Compatibilizers, Uses and Benefits in Polymer Blends,* Hanser, Munich, Vienna, New York, 1996.
18. A. Ghaffar, C. Sadrmohaghegh, and G. Scott, *Eur. Polym. J.,* **17,** 941 (1981).
19. C. Sadrmohaghegh, G. Scott, and E. Setoudeh, *Eur. Polym. J.,* **19,** 81 (1983).
20. D. S. Chiu, Z. Zhang, and G. G. Siu, *J. Reinf. Plast. Compos.,* **15,** 74 (1996).
21. Z. Zhang, D. S. Chiu, and G. G. Siu, *J. Reinf. Plast. Compos.,* **15,** 452 (1996).
22. P. H. Hermans and S. A. Weidinger, *Makromol. Chem.,* **50,** 98 (1961).
23. J. P. Trotignon and J. Verdu, *J. Appl. Polym. Sci.,* **34,** 1 (1987).
24. P. Zipper, A. Janosi, and E. Wrentschur, *J. Phys. IV Suppl. J. Phys. I,* **3,** 33 (1993).
25. P. Zipper, A. Janosi, E. Wrentschur, C. Knabl, and P. M. Abuja, *Öster. Kunststoff-Zeitschrift,* **24,** 162 (1993).
26. L. E. Alexander, *X-ray Diffraction Methods in Polymer Science,* Wiley, New York, 1969, p. 423.
27. G. M. Jordhamo, J. A. Manson, and L. H. Sperling, *Polym. Eng. Sci.,* **26,** 517 (1986).
28. S. L. Aggarwall, in *Processing, Structure and Properties of Block Copolymers,* M. J. Folkes, Ed., Elsevier, London, 1985, Chap. 1.
29. G. Radonjič, in *Proceedings of the European Symposium on Polymer Blends,* Maastricht, May 1996, p. 187.
30. G. Radonjič, V. Musil, and M. Makarovič, *Acta Chim. Sloven.,* **44,** 29 (1997).
31. G. Radonjič and V. Musil, *Angew. Makromol. Chem.,* **251,** 141 (1997).
32. L. Yang, T. G. Smith, and D. Bigio, *J. Appl. Polym. Sci.,* **58,** 117 (1995).
33. M. K. Akkapeddi and B. Van Buskirk, *Adv. Polym. Technol.,* **11,** 263 (1992).
34. S. Rabiej, *Eur. Polym. J.,* **29,** 625 (1993).
35. G. Radonjič, V. Musil, and I. Šmit, to appear.
36. J. W. Teh, A. Rudin, and J. C. Keung, *Adv. Polym. Technol.,* **13,** 1 (1994).
37. H. Saechtling, *International Plastics Handbook,* 2nd ed., Hanser, Munich, 1987, pp. 165, 185.
38. L. R. Lindsey and D. R. Paul, *J. Appl. Polym. Sci.,* **26,** 1 (1981).
39. L. E. Nielsen and R. F. Landel, *Mechanical Properties of Polymers and Composites,* 2nd ed., Marcel Dekker, New York, 1994, Chap. 7.
40. R. A. Dickie, in *Polymer Blends,* Vol. 1, D. R. Paul and S. Newman, Eds., Academic Press, New York, 1978, Chap. 8.
41. E. H. Kerner, *Proc. Phys. Soc.,* **B69,** 808 (1956).
42. Y. Sato and J. Furukawa, *Rubb. Chem. Technol.,* **35,** 857 (1962).
43. T. Kunori and P. H. Geil, *J. Macromol. Sci. Phys.,* **B18,** 93 (1980).
44. C. B. Bucknall, *Toughened Plastics,* Applied Science, London, 1977.
45. J. Karger-Kocsis, A. Kalló, A. Szafner, G. Bodor, and Zs. Sényei, *Polymer,* **20,** 37 (1979).